ELSEVIER

Chemical Geology 169 (2000) 299–318

CHEMICAL GEOLOGY
INCLUDING
ISOTOPE GEOSCIENCE

www.elsevier.com/locate/chemgeo

Mineral transformation associated with the microbial reduction of magnetite

Hailiang Dong [a,*], James K. Fredrickson [b], David W. Kennedy [b], John M. Zachara [b], Ravi K. Kukkadapu [b], Tullis C. Onstott [a]

[a] *Department of Geosciences, Guyot Hall, Princeton University, Princeton, NJ 08544, USA*
[b] *Pacific Northwest National Laboratory, Richland, WA 99352, USA*

Accepted 2 December 1999

Abstract

Although dissimilatory iron reducing bacteria (DIRB) are capable of reducing a number of metals in oxides and soluble forms, the factors controlling the rate/extent of magnetite reduction and the nature of the mineral products resulting from magnetite reduction are not well understood. This study was carried out to investigate mechanisms and biogeochemical processes occurring during magnetite reduction by the DIRB, *Shewanella putrefaciens* strains CN32 and MR-1. Reduction experiments were performed with biogenic and synthetic magnetite in well-defined solutions. Biogenic magnetite was generated via microbial reduction of hydrous ferric oxide (HFO). Biogenic magnetite in solutions buffered with either bicarbonate (HCO_3^-) or 1,4-piperazinediethanesulfonic (PIPES), with or without P, was inoculated with strain CN32 and provided with lactate as the electron donor. Synthetic magnetite in a bacteriological growth medium (M1) was inoculated with either aerobically or anaerobically grown cells of strain (CN32 or MR-1). Fe(II) production was determined by HCl extraction of bioreduced samples in comparison to uninoculated controls, and the resulting solids were characterized by X-ray diffraction (XRD), Mössbauer spectroscopy, scanning and transmission electron microscopy (SEM and TEM). The extent and rate of biogenic magnetite reduction in the bicarbonate-buffered medium was higher than that in the PIPES-buffered medium, via complexation of bioproduced Fe(II) with HCO_3^- (or PO_4^{3-}) and formation of siderite (vivianite). *S. putrefaciens* CN32 reduced more synthetic than biogenic magnetite with differences attributed mainly to medium composition. In the HCO_3^--buffered solutions, Fe(III) in the biogenic magnetite was reduced to Fe(II), and siderite precipitated. In the PIPES-buffered medium, Fe(III) in biogenic magnetite was also reduced to Fe(II), but no secondary mineral phases were observed. Vivianite formed in those solutions containing P and in all synthetic magnetite treatments where there was sufficient supply of P from the M1 medium. Electron microscopy and Mössbauer spectroscopy results suggest that the reduction process involves dissolution–precipitation mechanisms as opposed to solid state conversion of magnetite to vivianite or siderite. The aqueous medium, pH, strain type, and bacterial growth conditions all affected the extent of magnetite reduction. The ability of DIRB to utilize Fe(III) in crystalline magnetite as an electron acceptor could have significant implications for biogeochemical processes in sediments where Fe(III) in magnetite represents the largest pool of electron acceptor.

Keywords: *Shewanella putrefaciens*; Reduction; Magnetite; Siderite; Vivianite

* Corresponding author. Tel.: +1-609-258-2597; fax: +1-609-258-1274.
E-mail address: hailiang@princeton.edu (H. Dong).

0009-2541/00/$ - see front matter
PII: S0009-2541(00)00210-2

1. Introduction

In the past decade, interest in the biogeochemical transformations accompanying microbial iron reduction reactions has been increasing. Fe(III) may have been the first external electron acceptor of global significance in microbial respiration (Walker, 1987; Cairns-Smith et al., 1992; de Durve, 1995). Magnetite formation thought to be a result of Fe(III) oxide reduction by Fe reducing microorganisms has been used as a possible evidence for respiratory processes in the early evolution of the Earth (Walker, 1987; Vargas et al., 1998), for life on Mars (McKay et al., 1996) and for the presence of a deep biosphere in the terrestrial subsurface (Gold, 1992). The reduction of Fe(III) and Mn(IV) by some bacteria has been shown to be coupled to the oxidation of organic carbon or H_2 (Lovley et al., 1989; Lovley and Lonergan, 1990; Kazumi et al., 1995). Iron and manganese often play a significant role in controlling both redox balance and carbon cycling in sediments (Nealson and Saffarini, 1994). Because of the wide distribution of Fe(III) reducing bacteria, their activities have implications for not only natural biogeochemical processes but also the fate and transport of multivalent metals and radionuclides (Nealson and Little, 1997; Lovley, 1995). Toxic metallic and radionuclide contaminants often strongly adhere to Fe and Mn oxide/hydroxide surfaces in soils and subsurface materials. When Fe(III) reducing bacteria convert Fe(III) and Mn(IV) mineral forms to soluble species, associated inorganic contaminants may also be released (Francis and Dodge, 1990).

Both amorphous hydrous ferric oxide (HFO) and crystalline Fe oxides (goethite, magnetite, hematite) are reducible by Fe(III) reducing microorganisms (Arnold et al., 1988; Lovley and Phillips, 1987; Kostka and Nealson, 1995; Roden and Zachara, 1996; Little et al., 1997; Zachara et al., 1998; Fredrickson et al., 1998), but the mechanism(s) by which bacteria reduce solid phase Fe oxides are not well understood. Roden and Zachara (1996) reported that the rate and extent of microbial Fe(III) reduction was positively correlated with surface area of the oxides. Direct contact between cell and oxide surfaces appears to be necessary for microbial respiration and reduction (Arnold et al., 1988; Lovley and Phillips, 1988; Kostka and Nealson, 1995), a requirement that is implied for magnetite reduction and dissolution. Most previous studies have been based on analyses of batch culture experiments with few attempts to probe the microbe-oxide interface (Granthan et al., 1997). Recent studies have shown that certain Fe(III) reducing bacteria (*Geobacter metallireducens* and *Shewanella alga*) can use humic substances and quinones as electron acceptors to transfer electrons from the electron donor to the acceptor (Lovley et al., 1996, 1998), relieving the requirement for direct contact. Fredrickson et al. (1998) investigated the effect of anthraquinone-2,6-disulfonate (AQDS), a humic acid analog, on the extent and rate of Fe(III) reduction in HFO, and found that the presence of AQDS significantly increased the rate and extent of Fe(III) reduction. They also characterized the mineral products formed as a result of bacterial Fe(III) reduction in various solutions, and determined that the mineral products strongly depended on the composition of the solutions. In bicarbonate-buffered solutions more extensive reduction was observed, and siderite was a major end product. In 1,4-piperazinediethanesulfonic acid (PIPES)-buffered solutions, reduction was less extensive, and a fine-grained crystalline magnetite was dominant. The presence of P and AQDS also affected the biogenic mineral phases formed and the extent of reduction. Thermodynamic calculations predicted that magnetite should be a precursor to siderite formation, but no direct evidence for the phase conversion from magnetite to siderite was observed.

Magnetite, siderite and vivianite are common mineral products observed during Fe(III) reduction in the laboratory studies (Sparks et al., 1990; Lovley, 1991; Mortimer et al., 1997; Fredrickson et al., 1998), and are ubiquitous in natural environments (Emerson, 1976; Emerson and Widmer, 1978; Walker, 1984; Karlin et al., 1987; Maher and Taylor, 1988; Pye et al., 1990; Baedecker et al., 1992; Mortimer et al., 1997). Although a direct link can not be established between these laboratory-produced biogenic minerals and those observed in nature, several lines of evidence suggest that at least some proportion of these minerals present in natural environments are biogenic (Pye et al., 1990).

In this study, we examine the factors controlling the extent and rate of magnetite reduction. More importantly, we specifically focused on the micro-

scopic characterization of mineral phase transitions during microbial reduction of these oxides. Effort was made to examine bacteria–mineral interactions to gain insight into possible reduction mechanisms. We also examined the reduction of a synthetic magnetite by aerobically and anaerobically grown *S. putrefaciens* strains CN32 and MR-1 in medium M1 to extend the results by Kostka and Nealson (1995), and to investigate the nature of mineral products. Biogenic magnetite from the reduction of HFO (Fredrickson et al., 1998) and synthetic magnetite were used as oxide phases. We used HCl extraction to monitor Fe(II) production, and X-ray diffraction (XRD), Mössbauer spectroscopy, scanning electron microscopy (SEM) and transmission electron microscopy (TEM) to investigate the solid phase changes associated with the bacterial reduction of the Fe oxides.

2. Experimental procedure

2.1. Bacteria, Fe oxides and media

For the first experiment, i.e., reduction of biogenic magnetite, we followed the procedure of Fredrickson et al. (1998) using biogenic magnetite generated from the microbial reduction of HFO. For the second experiment, i.e., reduction of synthetic magnetite by aerobically and anaerobically grown CN32 and MR-1 cells in M1 medium, we used a procedure as that defined by Kostka and Nealson (1995). The first experiment was conducted using a defined medium identical to that used in previous experiments with HFO where magnetite was observed to be a stable end product of reduction in some PIPES-buffered treatments (Fredrickson et al., 1998). Results from the previous study showed that cell growth was not significant in the defined medium with HFO as the sole electron acceptor when inoculated with relatively high ($>10^8$ cells ml^{-1}) cell densities. The second experiment with synthetic magnetite was conducted with a complex growth medium (M1) to allow for better comparability with the findings of Kostka and Nealson (1995).

2.1.1. Reduction of biogenic magnetite by CN32

S. putrefaciens strain CN32 (DOE's Subsurface Microbial Culture Collection) was provided courtesy of Dr. David Boone (Portland State University). This strain was isolated from a subsurface core sample (250-m below the ground surface) obtained from the Morrison Formation in northwestern New Mexico. Strain CN32 is a Gram-negative, metal-reducing bacterium that can grow either aerobically or anaerobically using a range of electron acceptors.

The components used in the biogenic magnetite reduction experiments were similar to those used in earlier experiments with HFO (Fredrickson et al., 1998). Briefly, they were the following: 3 ml of a biogenic magnetite slurry, estimated final concentration of $\sim$100 mM total Fe, 10 mM Na lactate (electron donor), 28 mM NH_4Cl, 1.3 mM KCl, 0.78 mM nitrilotriacetic acid, 1.2 mM $MgSO_4 \cdot 7H_2O$, 1.7 mM NaCl, 0.29 mM $MnSO_4 \cdot H_2O$, 95 μM $ZnCl_2$, 36 μM $FeSO_4 \cdot 7H_2O$, 68 μM $CaCl_2 \cdot 2H_2O$, 42 μM $CoCl_2 \cdot 6H_2O$, 10 μM $Na_2MoO_4 \cdot 2H_2O$, 7.6 μM $Na_2WO_4 \cdot 2H_2O$, 10 μM $NiCl_2 \cdot 6H_2O$, 4 μM $CuSO_4 \cdot 5H_2O$,2.1 μM $AlK(SO_4)_2 \cdot 12H_2O$, 16 μM H_3BO_3. The medium was buffered with either 30 mM $NaHCO_3$ or 30 mM PIPES with or without 4.3 mM NaH_2PO_4. Medium was dispensed into 10-ml pressure tubes, purged with O_2-free N_2:CO_2 (80:20) for the bicarbonate-buffered medium or O_2-free N_2 for the PIPES-buffered medium, stoppered with butyl rubber closures, crimp sealed and autoclaved.

CN32 cells were grown aerobically and harvested by centrifugation from aerobic tryptic soy broth (TSB) cultures, washed with buffer to remove residual TSB, resuspended in bicarbonate or PIPES buffer, and purged with O_2-free N_2 or N_2:CO_2. Cells were added to the media to obtain a final concentration of $2–3 \times 10^8$ ml^{-1}. The biogenic magnetite from HFO (Fredrickson et al., 1998) was prepared using the following procedure. The biogenic magnetite was suspended in 1M Na acetate at pH 4.5–5, and extracted overnight at 30°C with agitation of 100 rpm to remove Fe(II) not associated with magnetite. Magnetite was then resuspended in 10% NaOH and shaken overnight at 65°C and 100 rpm to remove residual cells and cell debris. Due to concerns of magnetite oxidation, the biogenic magnetite was not autoclaved. However, the pre-treatment with NaOH would have effectively sterilized the magnetite by lysing the cells. Magnetite was washed twice in 0.1 M Na perchlorate for 1 h at 30°C and 100 rpm, resuspended in anaerobic water and then added to

the medium. The biogenic magnetite prepared in this manner was confirmed by XRD. The treatment tubes were incubated in the dark at 30°C and agitated at 100 rpm. Controls consisted of solutions that received 1 ml of anaerobic buffer in place of CN32 cell suspension. Chemical analyses of experiments with biogenic magnetite were conducted on duplicate samples while experiments with the synthetic magnetite were analyzed in triplicate. Separate sets of tubes were sacrificed at each time point for analysis (7 and 14 days).

2.1.2. Reduction of synthetic magnetite by aerobically and anaerobically grown CN32 and MR-1 in M1 medium

A synthetic magnetite was prepared using the procedure described by Schwertmann and Cornell (1991). The synthetic magnetite prepared in such a manner had a BET-measured surface area of 15 m^2 g^{-1}. The identity of the phase was confirmed by XRD and Mössbauer spectroscopy. The Fe(III)/Fe(II) ratio in an HCl-dissolved sample of this material was 2.6. Approximately 0.11 g of dried synthetic magnetite was placed into 10-ml pressure tubes, flushed with N_2, stoppered with butyl rubber closures, crimp sealed and autoclaved.

The M1 medium contained 10 mM lactate as the electron donor and various compounds to support cell growth. These compounds included the following: 0.02% yeast extract, 0.01% Bactopeptone, 9.0 mM $(NH_4)_2SO_4$, 5.7 mM K_2HPO_4, 3.3 mM KH_2PO_4, 2.0 mM $NaHCO_3$, 1.01 mM $MgSO_4 \cdot 7H_2O$, 0.485 mM $CaCl_2 \cdot 2H_2O$, 67.2 μM Na_2EDTA, 56.6 μM H_3BO_3, 10.0 μM NaCl, 5.4 μM $FeSO_4 \cdot 7H_2O$,5.0 μM $CoSO_4$, 5.0 μM $Ni(NH_4)_2(SO_4)_2$, 3.87 μM Na_2MoO_4, 1.5 μM Na_2SeO_4, 1.26 μM $MnSO_4$, 1.04 μM $ZnSO_4$, 0.2 μM $CuSO_4$, 20 mg l^{-1} arginine, 20 mg l^{-1} glutamate, and 20 mg l^{-1} serine. The pH was buffered at 6.2 by the addition of 100 mM HEPES [4-(2-hydroxyethyl)-1-piperazineethane sulfonic acid]. Sterile anaerobic M1 medium of 9 ml in volume was dispensed into the pressure tubes containing the magnetite in an anaerobic chamber.

CN32 and MR-1 cells were cultured either aerobically on TSB (without dextrose) for 16 h at 30°C with shaking at 100 rpm, or anaerobically on TSB with 40 mM fumarate for 40 h at 30°C without shaking. Cells were washed twice and centrifuged at 6000 rpm for 10 min in sterile PIPES buffer at pH 7, followed by one wash and re-suspension to $\sim 10^9$ cells ml^{-1} in M1 medium. Aerobically cultured cells of CN32 and MR-1 were added to the pressure tubes containing the synthetic magnetite and M1 medium to obtain a final concentration of 3×10^8 cells ml^{-1}. Anaerobically grown cells of CN32 and MR-1 were added to the tubes containing the magnetite and M1 medium to obtain a final concentration of 2.3×10^8 cells ml^{-1}. The total volume of medium in each tube, including magnetite and cells, was 10 ml. The magnetite in the medium had a final concentration of 48 mM. All treatment tubes were incubated in the dark at 30°C and agitated at 100 rpm until the end of the experiment. Controls consisted of tubes with magnetite and M1 medium without cells. All treatments with aerobically cultured cells were incubated for 14 days, and those with anaerobically cultured cells were incubated for 12 days.

2.2. Analyses of Fe(II) production

At select time points (14 days for the biogenic magnetite experiment, and 12–14 days for the synthetic magnetite experiment), replicate tubes were removed from the incubator, and transferred to an anaerobic ($Ar:H_2$, 95:5) glovebag. One tube was reserved for characterization of mineral products by XRD, SEM, TEM, and Mössbauer (synthetic magnetite only). Butyl rubber stoppers were removed from the two (biogenic magnetite) or three (synthetic magnetite) remaining tubes, and the solution pH was measured using a Ross combination electrode, and a mean value was obtained. One milliliter of suspension was removed from each tube, filtered through a 0.2-μm polycarbonate filter, and extracted by 1 ml of 0.5 N Ultrex HCl. This fraction was considered as the soluble fraction and analyzed for Fe(II) and phosphate. Due to concerns about artificially elevated soluble Fe(II) concentrations in the filtrate caused by the passage of nanometer-sized magnetite particles and cell-bound Fe(II) through the 0.2 μm filter, Fredrickson et al. (1998) used two different filter sizes, 0.2 μm and 0.002 μm, and found no difference in measured soluble Fe(II) concentration, demonstrating that a 0.2-μm filter was sufficient to filter Fe(II) solids for these experiments. HCl extractable Fe(II) was obtained by mixing 9 ml of 1 N

HCl with the 9 ml remaining suspension in each tube and equilibrating for ~48 h. After this period, the supernatant was removed from each tube, subsampled and diluted for Fe(II) and total Fe analyses. This extraction method was similar to that previously used to measure Fe(II) in microbially reduced magnetite suspensions (Kostka and Nealson, 1995) but differed from that method, which equilibrated 0.1 g or 0.1 ml of sample with 5.0 ml of 0.5 N HCl for 15 min before analyzing by ferrozine (Lovley and Phillips, 1986). Stronger acid, 6 N HCl, was used to dissolve the synthetic magnetite to obtain the initial Fe(III)/Fe(II) ratio of 2.6. Fe(II) in acidified filtrates (0.2 μm) or extracts was determined using the ferrozine assay (Lovley and Phillips, 1986). Phosphate concentrations were determined using an ammonium paramolybdate assay (Olsen and Sommers, 1982).

2.3. X-ray diffraction

Solid precipitate in the tube that was set aside at the end of the experiment was split for XRD, Mössbauer, and electron microscopic analysis. The solid material for XRD analysis was dried on a watch glass in an anaerobic chamber for 48 h. The dried solid was scraped off the watch glass onto a wax sheet, and then placed in a scintillation vial stored in an anaerobic atmosphere until the time of analysis. Immediately before analysis, a scintillation vial was opened and mineral product was transferred to a quartz XRD slide with a 9-mm I.D. zero background cavity. The XRD apparatus consisted of two Philips Wide-Range Vertical Goniometers with incident-beam 2-theta compensating slits, soller slits, fixed 2 mm receiving slits, diffracted beam graphite monochromators, and scintillation counter detectors. The X-ray source was a Philips XRG3100 X-ray Generator operating a fixed-anode, long-fine-focus Cu tube at 40 kv, 50 mA (1800 W). Instrument control was by means of Databox NIMBIM modules (Materials Data, Livermore, CA).

2.4. Scanning electron microscopy

The split for the electron microscopy was preserved in 5% glutaraldehyde and stoppered with rubber closures. All solid materials were prepared in an anaerobic glovebag to prevent oxidation of Fe(II) containing minerals. Individual grains of solids were dispersed onto holy-carbon Cu grids and allowed to dry in the glovebag. The Cu grids were carefully placed into serum vials with crimp seals for transport to the microscopes. The only exposure to air occurred during transfer from the serum vials to sample holder and chamber. Samples were examined by SEM to identify minerals and to obtain crystal morphology information using a Philips XL30 field emission gun (FEG) SEM fitted with backscatter and secondary electron detectors and IMIX energy dispersive X-ray analytical system. Qualitative energy dispersive spectrum (EDS) chemical analyses were obtained by focusing the beam to a spot over the target area.

2.5. Embedding, sectioning procedure and TEM

Cell-mineral suspensions were washed three times with 0.1 M Na cacodylate buffer at pH 7.2 followed by three washes with cold deionized water. Cell-mineral suspensions were fixed with 1% potassium ferricyanide reduced osmium tetroxide for 1 h on ice. The suspensions were then rinsed four times with deionized water, then stained overnight at room temperature with 1% aqueous uranyl acetate. The suspensions were rinsed again for three times with deionized water, dehydrated through graded series of ethanol and embedded in medium grade Spurr resin. Ultra-thin sections were cut (60–95 nm in thickness) with a Diatome diamond knife using a Reichert Ultracut E ultramicrotome. Sections were counterstained with Reynold's lead citrate and examined at 80 KV with a JEOL 100C TEM.

2.6. Mössbauer spectroscopy

Random orientation absorbers were prepared by mixing 17–28 mg of dried sample with petroleum jelly in a 0.5-in. or 3/8-in. thick and 0.5-in. I.D. Cu holder sealed at one end with clear scotch tape. The sample space was filled with petroleum jelly and the ends sealed with the tape. The bioreduced samples (synthetic magnetite sample reduced with aerobically grown bacteria) were handled under an anaerobic atmosphere. Spectra were collected at room temperature (RT) using ~50 mCi (1.85 MBq) ^{57}Co/Rh single-line thin sources. The Mössbauer bench (MB-500; WissEL, Germany) was equipped with a dual Mössbauer drive system to gather data simultane-

ously for two experiments. The velocity transducer (MVT-1000; WissEL) was operated in the constant-acceleration mode (23 Hz, ±10 mm/s). Data were acquired on 1024 channels and then folded to 512 channels to give a flat background and a zero-velocity position corresponding to the center shift (CS or δ) of a metallic-Fe foil at room temperature. Calibration spectra were obtained with a 20-μm thick α-Fe foil (Amersham, England) placed in exactly the same position as the samples to minimize any error due to changes in geometry. The transmitted radiations were recorded with Ar–Kr proportional counters. The unfolded spectra obtained were folded and evaluated with Recoil (University of Ottawa, Canada) program using Voigt-based hyperfine parameter distribution method (Rancourt and Ping, 1991).

3. Results

3.1. Effect of buffer type and phosphate on reduction of biogenic magnetite

The 0.5 N HCl dissolved the biogenic and synthetic magnetites in the unincoculated controls to varying degrees (Table 1), probably due to differences in the degree of crystallinity, particle size and surface area. The amount of Fe(II) that was extracted by 0.5 N HCl in these samples, therefore, included biologically reduced Fe(II) in addition to Fe(II) associated with the original magnetite sample. As the reduction of magnetite increased, the proportion of magnetite Fe(II) released would have increased accordingly. Therefore, it is not possible to precisely determine the actual mass of magnetite Fe(III) that was reduced by the microorganisms. Regardless, the amount of 0.5 N HCl-extractable Fe(II) in the bioreduced magnetite samples was 1.5- to 1.7-fold greater than the Fe(II) in the unreduced (uninoculated control) magnetite (Table 1) indicating extensive reduction. The extent of reduction depended on the medium, with the bicarbonate-buffered media promoting greater Fe(III) reduction than the PIPES-buffered media. The concentration of $Fe(II)_{aq}$ was highest in the PIPES buffer, lower in the PIPES + P and lowest in the bicarbonate buffered medium and uninoculated controls (Table 1). These differences correspond to the presence of inorganic ligands, phosphate and bicarbonate, that can complex and precipitate Fe(II). The presence of phosphate did not significantly enhance the reduction and, in fact, microbial reduction of magnetite in the bicarbonate-

Table 1
The extent of magnetite reduction, mineral products and solution composition in various treatments

Treatment	0.5 N HCl Fe(II) (mM)	Post-reduction minerals[a]	Aqueous Fe(II) (mM)	Aqueous P (mM)	Final pH
Biogenic magnetite[b]					
HCO_3	54.1 (1.3)[c]	Siderite	0.04 (0.01)	–	7.4
HCO_3 + P	51.3 (2.7)	Siderite, vivianite	0.04 (0.01)	bd[d]	7.4
PIPES	45.2 (2.0)	None	0.84 (0.05)	–	7.0
PIPES + P	49.4 (1.3)	None	0.41 (0.02)	Bd	7.1
Uninoculated HCO_3 + P	31.3	–	0.04	0.79	7.0
Uninoculated PIPES + P	29.7	–	0.07	0.49	7.0
Synthetic magnetite[e]					
Aerobically grown CN32	22.3 (1.9)	Vivianite	0.32 (< 0.01)	1.25 (0.03)	6.4
Aerobically grown MR-1	15.8 (4.3)	Vivianite	0.24 (0.04)	2.74 (0.45)	6.4
Anaerobically grown CN32	18.6 (3.9)	Minor vivianite	0.47 (0.02)	1.83 (0.22)	6.4
Anaerobically grown MR-1	6.4 (1.8)	Minor vivianite	0.40 (0.04)	7.22 (1.24)	6.3
Uninoculated control	2.8	–	0.01	8.50	6.2

[a] Mineral (other than magnetite) identification was based on XRD, SEM and Mössbauer spectroscopy.
[b] Each treatment was incubated for two time points (7 and 14 day, respectively).
[c] Values in parentheses are standard deviations of the means of three replicates.
[d] bd = below detection.
[e] All treatments with aerobically cultured cells were incubated for 14 days, and those with anaerobically cultured cells were incubated for 12 days.

buffered medium with phosphate was less than its equivalent treatment without phosphate.

3.2. Bioreduction of synthetic magnetite

The initial Fe(III) concentration in the synthetic magnetite was measured by sequential extraction of 0.5 N HCl followed by 6 N HCl. As expected, 0.5 N HCl only partially dissolved the synthetic magnetite whereas the 6 N HCl promoted complete dissolution. The Fe(III)/Fe(II) ratio was 2.6 as determined by the 6 N HCl dissolution analysis. Mössbauer spectroscopy (see Section 3.5.1.) confirmed Fe(III)/(II) ratio of 2.6 and the identity of the synthetic Fe oxide as magnetite but indicated that it was slightly oxidized in comparison to stoichiometric magnetite with an Fe(III)/(II) ratio of 2.0.

Aqueous Fe(II) was insignificant compared with 0.5 N HCl extractable Fe(II) in this experiment (Table 1). There was no appreciable difference in aqueous Fe(II) concentrations among the various bioreduced treatments as they ranged from 0.24 to 0.47 mM but all were much higher than in uninoculated control, which was 0.01 mM $Fe(II)_{aq}$. The overall extent of reduction, as measured by 0.5 N HCl extractable Fe(II) in the microbially reduced treatments relative to an uninoculated control, was greater in the treatments with aerobically grown CN32 and MR-1 cells than that in the treatments with cells grown anaerobically with fumarate (Table 1). Under the same condition, CN32 cells reduced more magnetite than MR-1 cells (Table 1). The effect of strain type on the extent of reduction was particularly pronounced in the treatments with anaerobically grown cells, where CN32 reduction resulted in approximately three times more HCl-extractable Fe(II) than MR-1 (Table 1).

The concentration of $PO_4^{3-}{}_{(aq)}$ in the treatments with anaerobically cultured cells was higher than that

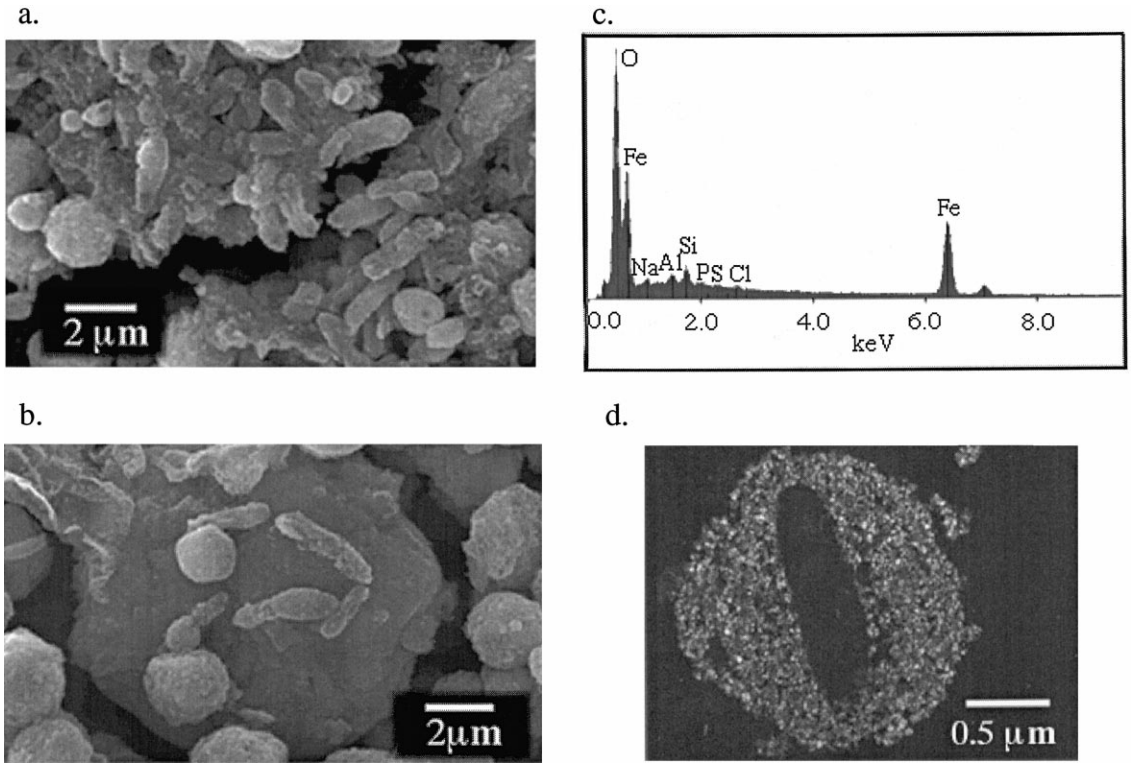

Fig. 1. (a, b) SEM image of CN32 cells on biogenic magnetite. (c) EDS spectrum from these cells revealing that they were coated by magnetite. (d) High resolution TEM micrograph showing direct contact between cell and magnetite. EDS spectrum was obtained from one of the cells on the low right corner of (a).

in the treatments with aerobically cultured cells (Table 1). In the treatments with anaerobically cultured cells, the concentration of soluble PO_4^{3-} was four times higher in the MR-1 than in the CN32 treatment. Low $PO_{4\,(aq)}^{3-}$ corresponded to high 0.5 N HCl extractable Fe(II), implying the formation of vivianite $[Fe_3(PO_4)_2 \cdot 8H_2O]$. It was expected therefore, that more vivianite formed in the CN32 treatment than in the MR-1 treatment. However, XRD, Mössbauer, and SEM data did not support this expectation (see below).

The 0.5 N HCl extractability of the starting and residual synthetic magnetite was assumed to be the same for all treatments and is supported by the Mössbauer spectroscopy results that indicate little or no structural change in the magnetite remaining after bioreduction.

3.3. Biogenic magnetite–cell interactions

Initial reduction proceeded via intimate association between bacterial cells and magnetite (Fig. 1a,b) as expected for enzymatic mediation of electron transfer to Fe oxides. Individual bacteria in the micrograph are rod-shaped (2.4 μm × 0.6 μm), but the EDS analyses of the cells gave rise to a magnetite composition, rather than an organic composition (Fig. 1c). TEM microscopy (Fig. 1d) confirmed the SEM observation that individual bacteria were in direct contact with magnetite crystallites. The nanocrystalline biogenic magnetite formed a spherical aggregate around the outside of individual cells. Cell membrane and internal structures were not clear in the image, possibly due to a shadowing effect from the magnetite crystals, blockage of stain penetration

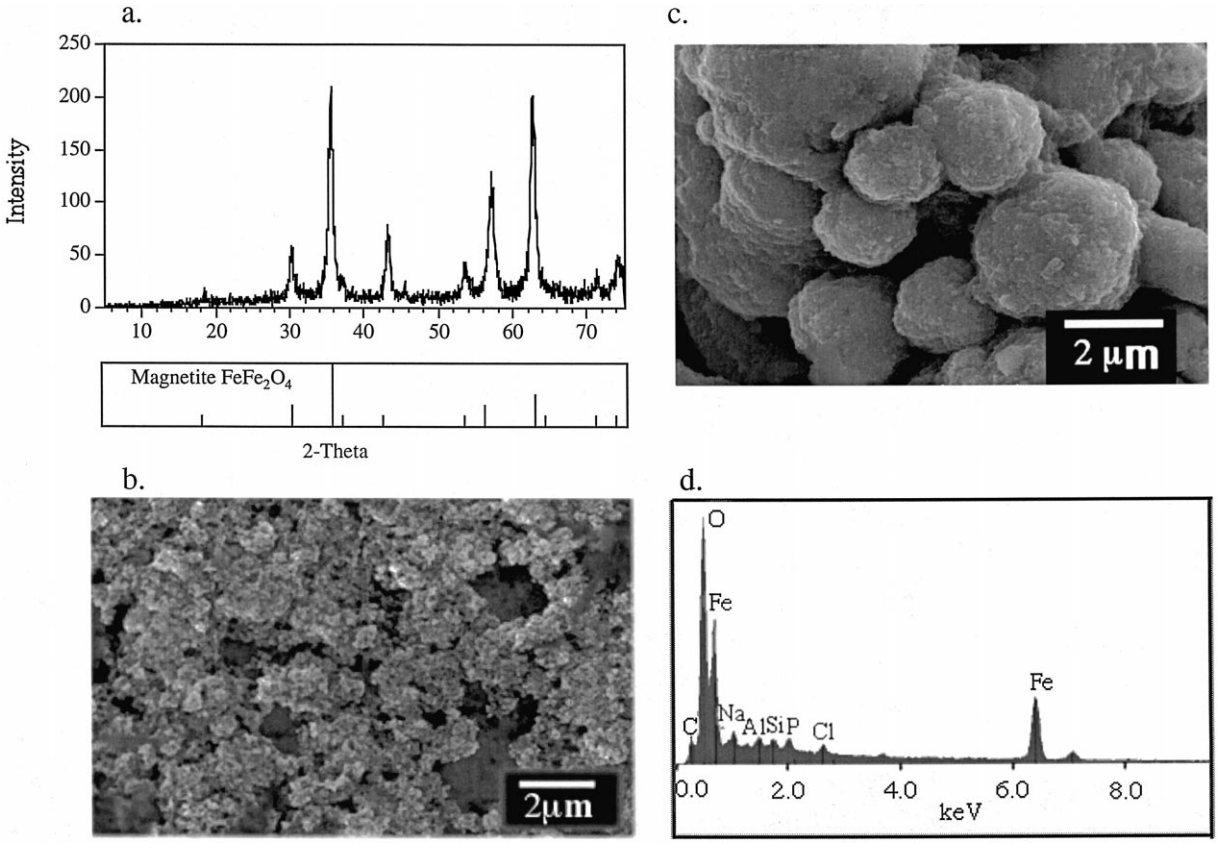

Fig. 2. (a) XRD pattern of the control in the bicarbonate buffer. (b, c) SEM images of the same control for 7 and 14 days, respectively. (d) EDS spectrum for the 7-day treatment with EDS target area from (b).

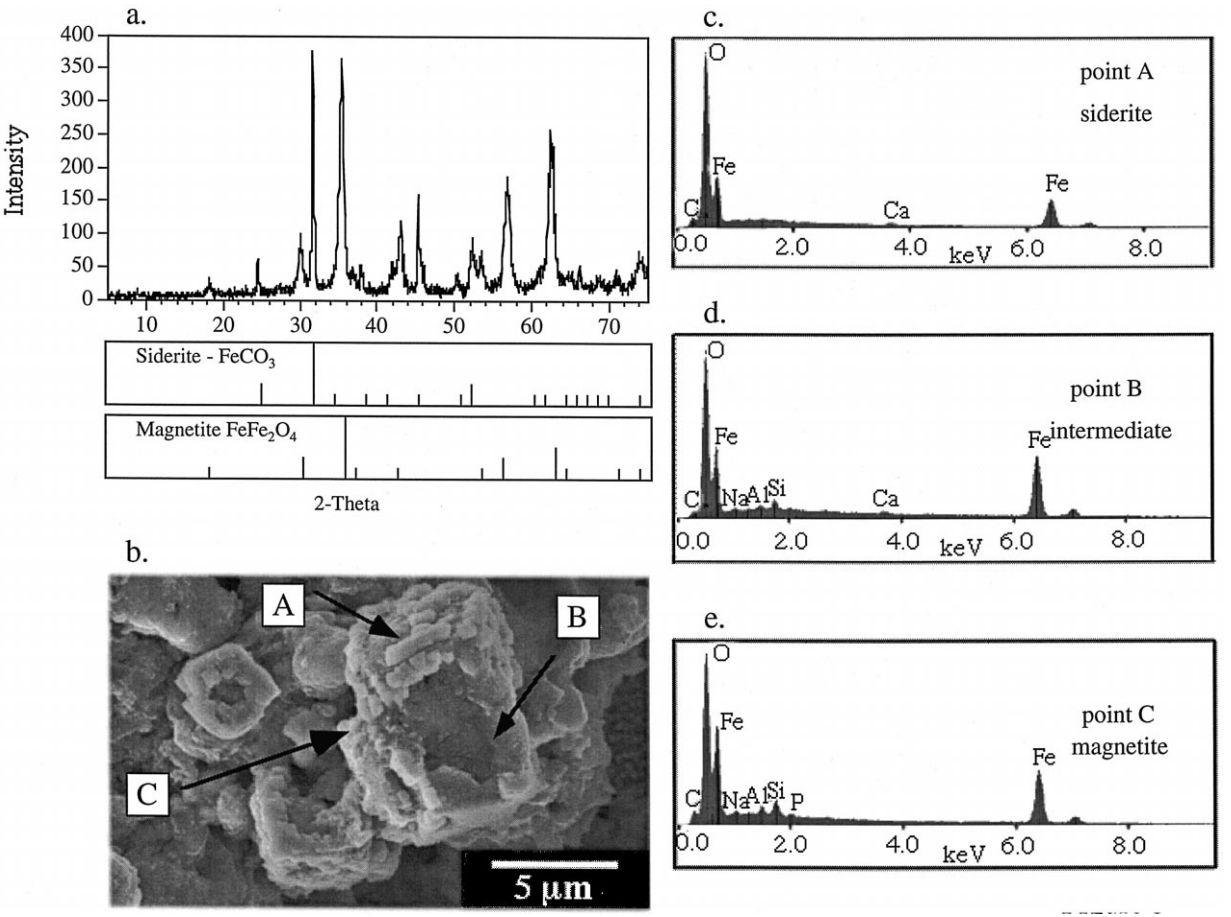

Fig. 3. (a) XRD pattern of the mineral solids from the bicarbonate-buffered medium showing that it consisted of siderite and magnetite. (b) SEM image of the same sample showing siderite precipitation on the base of magnetite. (c, d, e) Three EDS spectra from the three points in (b) showing different compositions.

by the magnetite coating or possibly lysis of cells before or during fixation. The latter is less likely because of the retention of the rod shape; lysis of the cell wall and membrane would be expected to result in spheroidal, as opposed to rod, morphologies. The magnetite coating was not of equal thickness, with bacterial ''polar regions'' being thinner (0.1–0.2 μm) than near the midsection (0.5–0.7 μm). Pore spaces were evident in the bio-induced magnetite aggregate, suggesting that the magnetite was probably held in place by a bacterial polymer. Although a quantitative analysis was not made, it appeared that porosity was the greatest in the regions adjacent to the cell surface, possibly suggesting these as more active regions of magnetite dissolution.

3.4. Mineral products of biogenic magnetite reduction by CN32

3.4.1. Bicarbonate-buffered solutions

In the control, magnetite was the only solid phase observed (Fig. 2). There was a change in morphology of the magnetite, however, between the 7- and 14-day incubation period. In the 7-day sample, the magnetite appeared as thin sheets of aggregates (Fig. 2b). In the 14-day sample, the magnetite appeared as globules, consisting of aggregates of individual nanometer-sized crystals (Fig. 2c). In all treatments, but in varying amounts, magnetite remained at the end of the incubation period. In some treatments (mainly in the PIPES-buffered solution), magnetite was the only solid phase observed, in spite of significant microbial reduction of Fe(III). Mineral products formed as a result of magnetite reduction in the bicarbonate-buffered solutions were morphologically diverse.

In the bicarbonate-buffered solution without P, siderite ($FeCO_3$) and magnetite (Fe_3O_4) were the predominant solid phases present after incubation (Fig. 3a). Siderite was more commonly observed in the 14 day-samples than in the 7 day-samples. Siderite was typically present as imperfect, small rhombohedral (pseudo-cubic) crystals of slightly different sizes (Fig. 3b). These crystals had precipitated on a fine-grained magnetite base (large crystal on the right in Fig. 3b). In some cases, the siderite had covered one-half of the magnetite base (low left in Fig. 3b). When these siderite crystals merged, they produced a larger, but still imperfect rhombohedral siderite crystal. Hollow internal structures (small crystal on the left in Fig. 3b) were often observed in the siderite. The three crystals in Fig. 3b represent three different stages of magnetite–siderite transformation that were commonly observed. Prior to siderite precipitation, the base magnetite appeared to have adjusted its morphology to accommodate for siderite deposition (Fig. 4a). As precipitation proceeded, an imperfect and large crystal of siderite resulted (Fig. 4b).

The EDS analyses revealed that the individual siderite crystals possessed a siderite composition (point A, Fig. 3c). The composition of siderite was characterized by the O/Fe peak ratio of approximately 3.5 and presence of a minor amount of Ca, presumably in solid solution with Fe in the structure. The composition of the fine-grained base magnetite varied from that of magnetite (point C, Fig. 3e) to intermediate between siderite and magnetite (point B, Fig. 3d). The magnetite composition was charac-

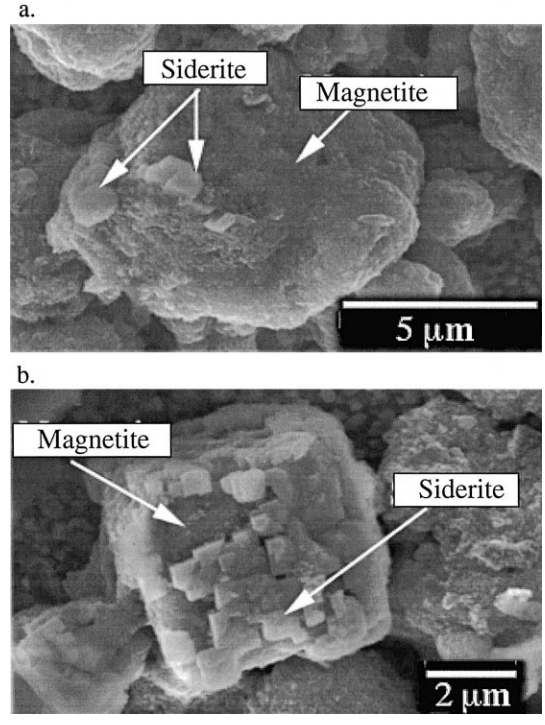

Fig. 4. (a) SEM image showing early stage of siderite precipitation to the magnetite base. (b) SEM image showing that siderite almost covered the magnetite base.

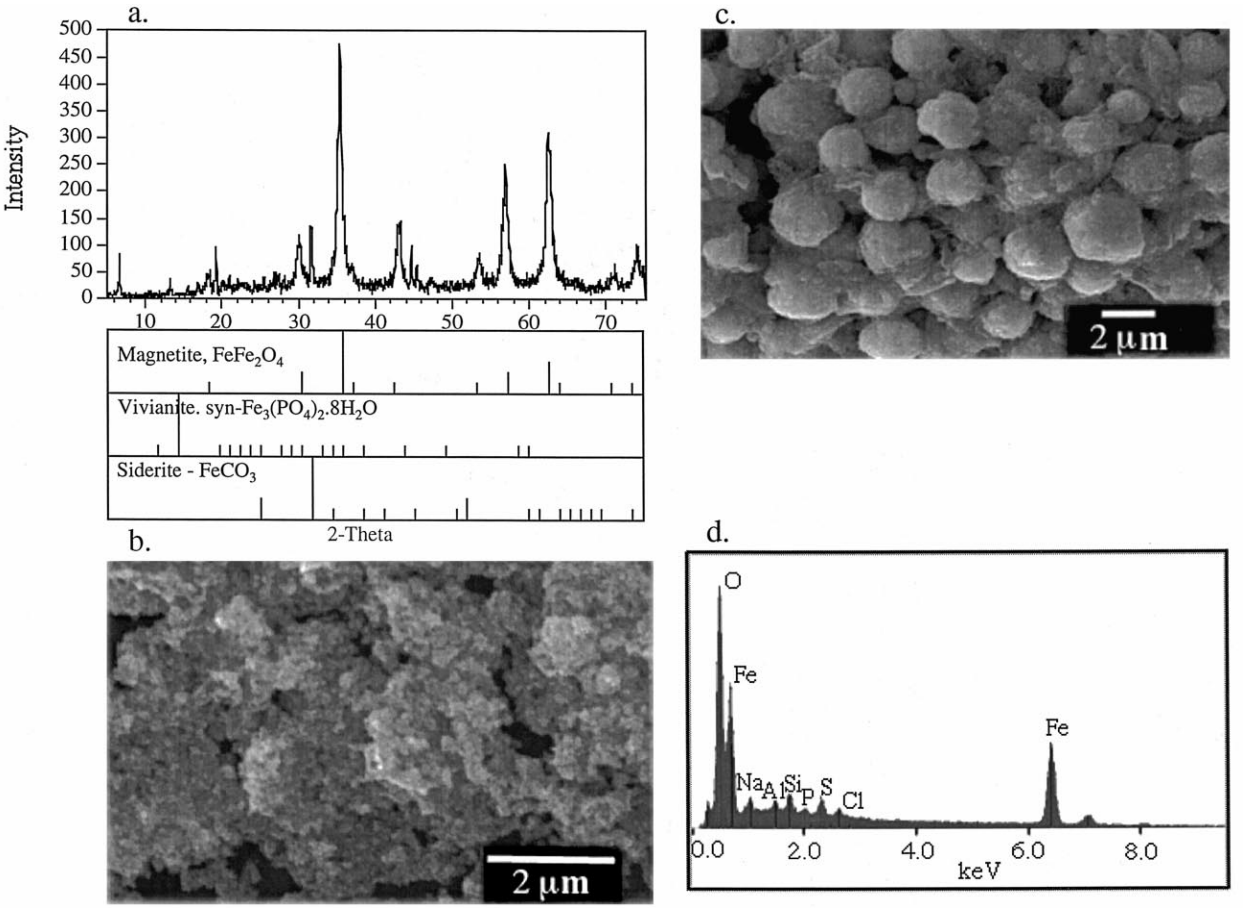

Fig. 5. (a) XRD pattern of the solid in the PIPES-buffered medium showing that the magnetite was the dominant phase. (b, c) SEM images of magnetite showing a change in morphology from thin sheets (7 days) to globules (14 days). (d) EDS spectrum obtained from one of the globules in (c).

terized by the O/Fe peak ratio of 2.3 and complete absence of Ca (Fig. 3e). The intermediate composition was characterized by the O/Fe peak ratio of approximately 2.8 and intermediate amount of Ca. In general, the base magnetite adjacent to siderite crystals possessed a composition closer to that of siderite.

In the bicarbonate-buffered medium with P, XRD detected the presence of siderite, vivianite and unreduced magnetite (data not shown). Siderite occurred as rhombohedral crystals ~ 2 μm in size. Vivianite occurred as tabular crystals 10–15 μm in size. The EDS analyses of vivianite revealed that Fe, P, and O were the dominant elements.

3.4.2. PIPES-buffered solution

A trace amount of vivianite was observed under SEM in the PIPES-buffered control with P, suggesting that abiotic formation of vivianite was possible but insignificant within time frame of the experiments (14 days). In the PIPES-buffered solution without P, XRD indicated that the majority of solid was unreduced magnetite, possibly with a small amount of siderite ($< 5\%$, Fig. 5a). In this case, phosphorus may have come from cells. Cell lysing could have released some amount of P. Siderite, however, was not detected by SEM (Fig. 5b,c). The lack of Fe(II) precipitate in this buffer suggested that the bioproduced Fe(II) sorbed to the unreduced magnetite, cells, or cell polymers because the aqueous concentration of Fe(II) was much less than that extracted by 0.5 N HCl. Alternatively, an amorphous phase of indistinct morphology may have formed, particularly at the cell–magnetite interface (Fig. 1d). During the course of the incubation in PIPES buffer

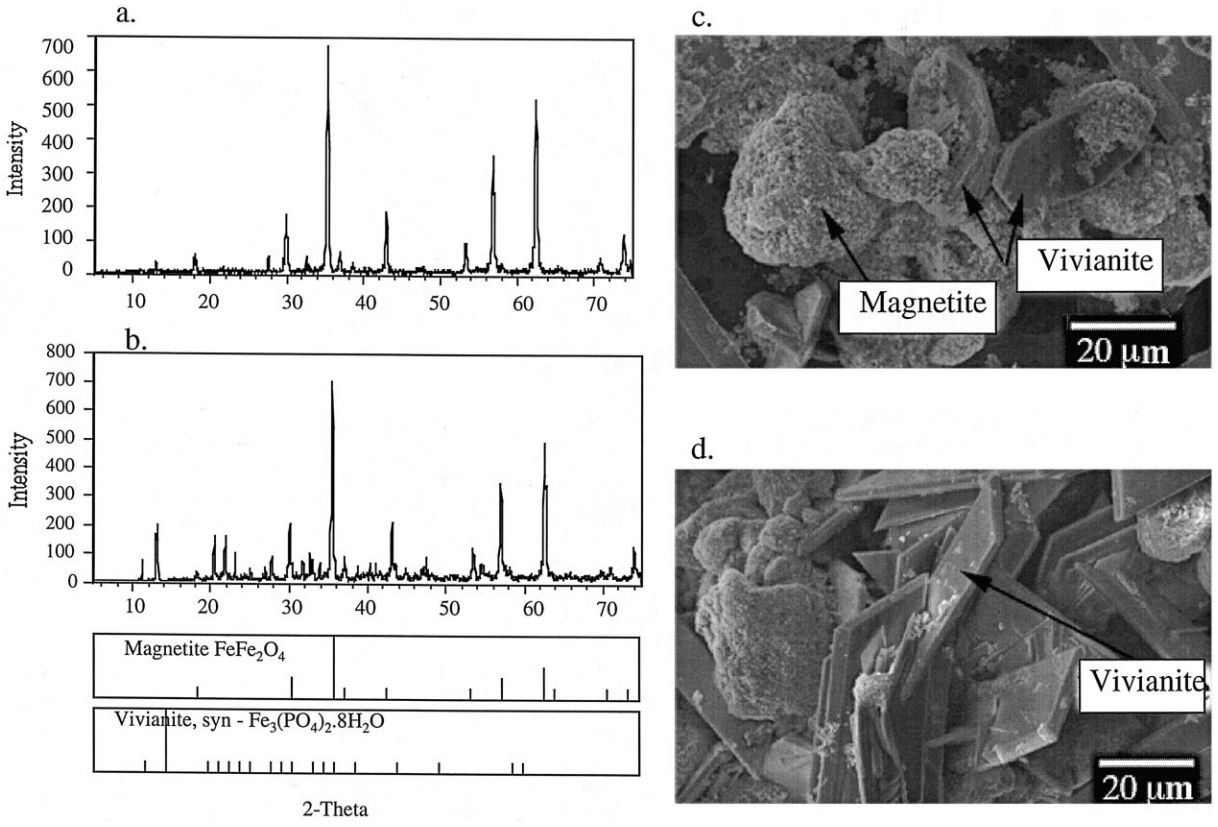

Fig. 6. (a, b) XRD patterns of the mineral solids from the treatments with aerobically grown CN32 and MR-1 on synthetic magnetite showing that the solids consisted of magnetite and vivianite. (c) SEM image of vivianite and unreduced magnetite from the CN32 treatment showing bladed and fibrous morphology of vivianite. (d) SEM image of vivianite and unreduced magnetite from the MR-1 treatment showing bladed morphology of vivianite.

(14 days), the morphology of magnetite changed dramatically from thin aggregate sheets at 7 days (Fig. 5b) to individual 2-μm spheres at 14 days (Fig. 5c). When P was present in the PIPES-buffered medium, a minor amount of vivianite formed but magnetite remained a major constituent in the solid material. Vivianite abundance could not account for all biogenic Fe(II) (~ 14%), suggesting that biogenic Fe(II) that was not present in the aqueous phase was associated with cell or oxide surfaces.

3.5. Mineral products of synthetic magnetite reduction by CN32 and MR-1

3.5.1. Electron microscopy

The synthetic magnetite was more crystalline than the biogenic magnetite as revealed by the higher signal to noise ratio of the former phase in XRD patterns (not shown). The mineral products were less diverse than those in the biogenic magnetite experiment, primarily because of uniformity of the medium composition. Following reduction, magnetite remained the dominant mineral in the solid phase, with various amounts of vivianite in different treatments. Overall, more vivianite was produced in the treatments with aerobically cultured cells than in the treatments with anaerobically grown cells (Figs. 6 and 7). This observation was consistent with the higher 0.5 N HCl extractable Fe(II) in the treatments with aerobically cultured cells. In the treatments with aerobically cultured cells, vivianite was more abundant in the treatment with the CN32 than in the treatment with the MR-1. Both incrusting bladed and fibrous vivianite crystals ~ 20 μm in the longest

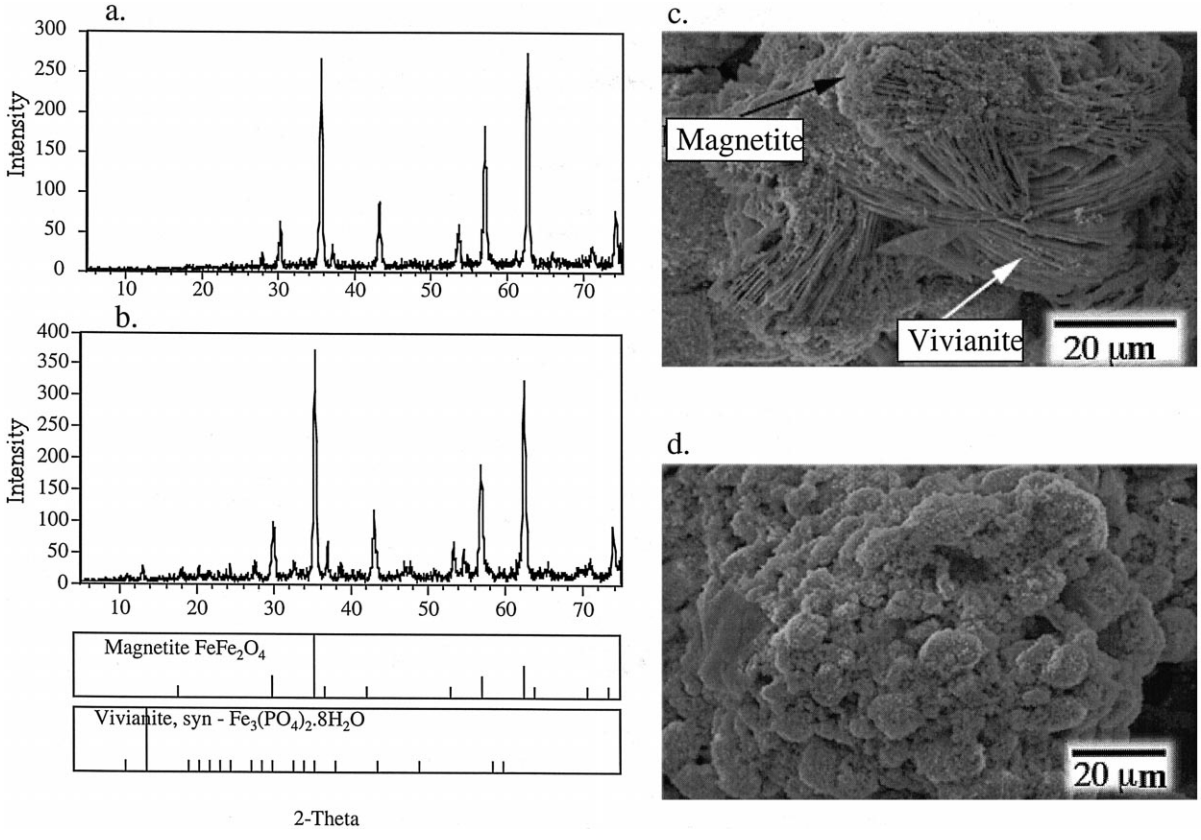

Fig. 7. (a, b) XRD patterns of the mineral solids from the treatments with anaerobically grown CN32 and MR-1 on magnetite showing little evidence for biomineralization in the bulk sample. (c) SEM image of the solid from the CN32 treatment showing fibrous vivianite. (d) SEM image of the solid from MR-1 the treatment showing predominantly magnetite.

dimension were observed in the CN32 treatment, and only bladed vivianite crystals ~20–30 μm in the longest dimension were present in the MR-1 treatment (Fig. 6c,d). With the anaerobically cultured cells, CN32 produced a small amount of vivianite (Fig. 7c,d). Although vivianite was not observed by SEM in the treatment with anaerobically grown MR-1 cells, the XRD pattern indicates that a small amount of vivianite was present. While P consumption by cells can not be ruled out, 6.0 to 7.4 mM P was recovered in the 0.5 N HCl extracts (data not shown). Only soluble and vivianite-associated P would be removed by this extraction, cell bound P (associated with lipids, nucleic acids etc.) would not. Thus, there was a maximum P consumption by cells of ~3 mM with the remaining P (not in the aqueous phase) potentially consumed by vivianite precipitation.

3.5.2. Mössbauer spectroscopy

^{57}Fe transmission Mössbauer spectroscopy was employed to characterize nature of the synthetic magnetite before and after bioreduction and to identify nature of any biogenic Fe^{2+} minerals formed. Mössbauer is a very sensitive and Fe specific technique with greater sensitivity than XRD; small amounts of Fe, as little as 1 wt.%, are identifiable by Mössbauer. In contrast to XRD, it provides information on compounds that do not exhibit long-range structural order (poorly crystalline materials) (Bancroft, 1973). Common Fe minerals such as siderite and vivianite are readily distinguished from each other and from magnetite, goethite, etc. (Greenwood and Gibb, 1971).

Experimental and simulated RT Mössbauer spectra of the unreduced and bioreduced synthetic magnetite samples are shown in Fig. 8. The spectra exhibited two sextets [and a doublet(s) in the bioreduced samples] that can be attributed to Fe^{3+} and $Fe^{2.5+}$ [average of Fe^{3+} and Fe^{2+} sensed by the Fe_{OCT}. nuclei due to rapid electron exchange between these Fe sites] sites. The Mössbauer parameters of the unreduced sample (Fig. 8a) [Fe^{3+}-hyper-

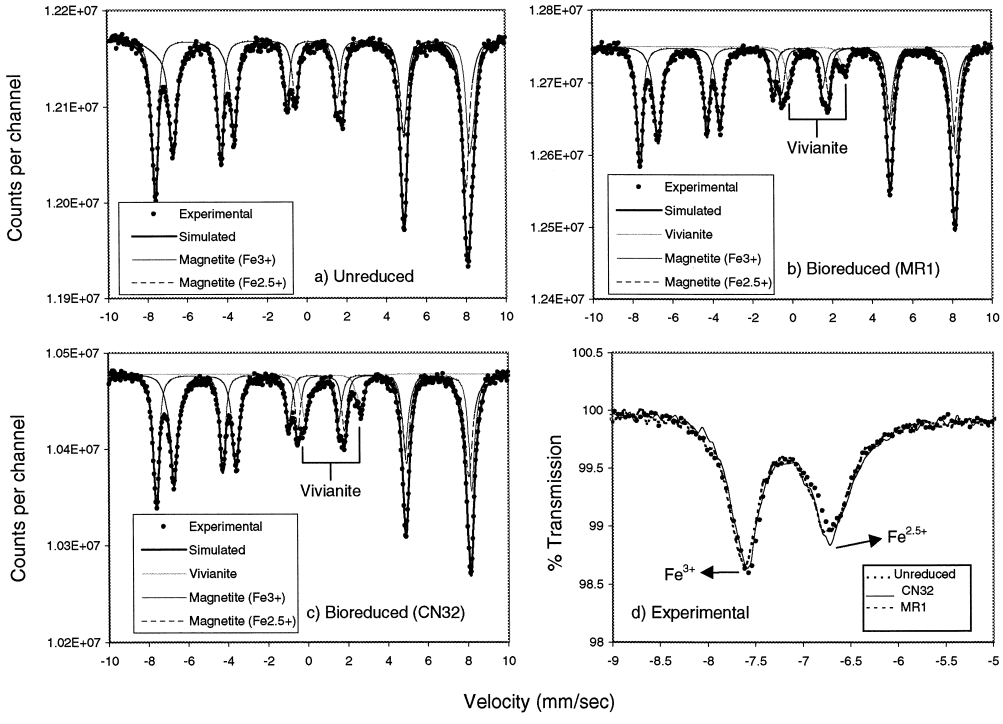

Fig. 8. (a) Experimental and simulated Mössbauer spectrum of the unreduced synthetic magnetite. (b, c) Experimental Mössbauer spectra of the synthetic magnetite sample treated with aerobically grown MR1 and CN32 bacteria, respectively. (d) Overlaid plots showing experimental Fe^{3+} (line 1) and $Fe^{2.5+}$ (line 1) lines of the unreduced and the bioreduced samples.

fine field (HF) of 49.2 T and $Fe^{2.5+}$-HF of 45.9 T] are similar to those previously described for pure magnetite (Greenwood and Gibb, 1971). The ratio of the relative area of the $Fe^{2.5+}$ sextet to the Fe^{3+} sextet (ρ or $Fe^{2.5+}/Fe^{3+}$ ratio), however, deviated significantly from pure magnetite, exhibiting a ratio of 1.10 in comparison to 1.80 expected for pure magnetite (Vandenberghe et. al., 1998). These results indicate limited oxidation of the synthetic magnetite since oxidation of $Fe^{2+}_{OCT.}$ lowers ρ. The newly generated $Fe^{3+}_{OCT.}$ has Mössbauer parameters similar to Fe^{3+}_{TET} hence, lower ρ. Although the synthetic material is clearly pure magnetite with no other phases such as maghemite or hematite, it should be considered a partially oxidized or non-stoichiometric magnetite. The Fe^{3+}/Fe^{2+} mole ratio of 2.64 obtained by rough estimation from the Mössbauer data is in good agreement with the Fe^{3+}/Fe^{2+} ration of 2.6 obtained by HCl dissolution.

The ρ of the bioreduced samples are similar to the unreduced sample [ρ(MR1) = 1.07, and ρ(CN32) = 1.18] as indicated by the coincidence of the outermost peaks of the unreduced and the bioreduced samples (Fig. 8d). In addition, the other Mössbauer parameters of the bioreduced samples are similar to the unreduced sample (Fig 8b,c). These results indicate that the remaining magnetite in the bioreduced samples was identical in composition to that in the starting material.

Simulation of the bioreduced samples indicated that approximately 6.5–8.2 spectral area is due to biogenic vivianite [$Fe_3(PO_4)_2 \cdot 8H_2O$]. Paramagnetic doublet(s) in Fig. 8b,c are attributable to vivianite. Mössbauer parameters of the doublet(s) are similar to vivianites reported in the literature (Greenwood and Gibb, 1971).

4. Discussion

4.1. Cell–magnetite interactions

The transformations in these experiments proceeded via a direct reduction of biogenic or synthetic magnetite Fe(III) by the *S. putrefaciens* as an electron acceptor during respiration (Fig. 1). Although it has been previously shown that *S. putrefaciens* can extensively reduce magnetite and that direct contact between bacteria and oxides is required for reduction (Kostka and Nealson, 1995), the fate of Fe(II) generated during magnetite reduction and the interactions between bacterial cells and mineral surfaces are unknown. TEM observations revealed aggregation/attachment of magnetite crystals around the cell periphery, suggesting binding via an extracellular polymer, possibly exopolysaccharide (EPS). Nealson and Little (1997) reported that *S. putrefaciens* formed a layer of EPS, obscuring individual cell morphology when viewed by an environmental SEM. Other studies have suggested or observed that *Shewanella* cells attach to solids via EPS (Obuekwe et al., 1981; Arnold et al., 1988). Based on SEM imaging and staining with ferritin, *S. alga* BrY produced EPS in response to Fe oxides (Urrutia and Fredrickson, unpublished data). Extracellular polymers produced by bacteria can extend out to 10 μm from the cell surface and can bind quantities of metal cations as high as 25% by weight (Geesey and Jang, 1989). We speculate that exopolymers may contribute significantly to the Fe(II) sorption capacity in these experiments, particularly in the PIPES-buffered suspensions where millimolar levels of 0.5 N HCl extractable Fe(II) were generated as a result of reduction yet only a fraction of the Fe(II) was in the aqueous phase. Whether extracellular polymers such as EPS have any role in attachment or reduction of magnetite or other Fe oxides by *S. putrefaciens* is unknown at this time. Further research is required to fully assess the role of cell surfaces and extracellular polymers in the attachment to Fe oxides and their role in reduction processes.

4.2. Microbial respiration and magnetite reduction

The extent of biogenic magnetite Fe(III) reduction in the bicarbonate-buffered solution was only slightly greater than that in the PIPES-buffered medium (Table 1). This result was somewhat intermediate between the previous findings by Roden and Zachara (1996) in experiments examining goethite reduction by *S. alga* BrY and those by Fredrickson et al. (1998) in their HFO reduction by *S. putrefaciens* CN32. Fredrickson et al. (1998) demonstrated that the bicarbonate-buffered medium promoted the microbial reduction of HFO relative to the PIPES-buffered medium most likely because bicarbonate

was able to complex with bioproduced Fe(II), and precipitate as siderite, effectively acting as a sink for Fe(II) removal. In the PIPES-buffered medium, magnetite was the primary precipitate, rendering two-thirds of Fe(III) potentially unavailable for further reduction.

In the current magnetite reduction experiment, siderite was observed as a primary solid phase in the bicarbonate-buffered medium. In contrast no crystalline Fe(II) precipitates were detected in the PIPES-buffered medium, suggesting Fe(II) association with the residual magnetite surface or possibly cellular material. Sorption of Fe(II) onto magnetite (or other amorphous precipitates) and cell surfaces may impede further reduction, resulting in an overall lower extent of reduction. Fe(II) binding to oxide or cell surfaces has previously been shown to retard the rate and extent of microbial reduction of Fe oxides (Roden and Zachara, 1996; Urrutia et al., 1998). The lower extent of Fe(III) reduction in the PIPES-buffered medium compared to the bicarbonate buffer (Table 1) suggests that, within the experiment duration, bioproduced Fe(II) may have had an inhibitory effect. Additional research is needed to precisely determine the fate of Fe(II) generated during microbial magnetite reduction in these experiments.

Previous experiments investigating the bioreduction of HFO by CN32 demonstrated that magnetite was a stable end product in PIPES-buffered medium (Fredrickson et al., 1998). The reasons for the reduction of biogenic magnetite in pH 7 PIPES lacking bicarbonate or P are unclear but may be due to the capacity of bacterial surfaces to bind Fe, as mentioned above. The surfaces of gram-negative bacteria are particularly effective at binding metal cations (Ferris, 1989) and fresh cultures of *S. alga* BrY have a Fe(II) sorption capacity of 0.1 mmol g^{-1} dry cells (Urrutia et al., 1998); *S. putrefaciens* CN32 would be expected to have a similar affinity for Fe(II). The affinity of cell surfaces, including EPS, for Fe (both II and III) would likely promote the bioreduction of magnetite by making the reaction more thermodynamically favorable, analogous to the effect of pH and complexing ligands. Unfortunately, quantification of the effect of cell surfaces on magnetite reduction is not possible at this time. Removal of possibly adsorbed Fe(II) from biogenic magnetite produced from our previous HFO reduction (see method section) would also expose fresh magnetite surfaces for further reduction.

The extent of the reduction of the synthetic magnetite was also influenced by *S. putrefaciens* strain. CN32, in general, reduced more magnetite than MR-1. This effect was more pronounced in the anaerobically grown cell treatments, where CN32 reduced fourfold more magnetite than MR-1. Different strains of *S. putrefaciens* apparently exhibit variable capacities for reducing magnetite. The reasons for differences between these two cultures are unclear. The differences in the extent of reduction between the biogenic and the synthetic magnetite can be attributed mainly to differences in Fe(III) content of the starting oxides and medium pH, 7.0 and 6.2, respectively, for the biogenic and synthetic magnetite reduction experiments.

There was evidence of vivianite precipitation in all magnetite reduction experiments with M1 medium that initially contained 9 mM PO_4^{3-}. The presence of vivianite combined with the low concentrations of soluble PO_4^{3-} (with the exception of anaerobically grown MR-1 cells) at the end of the experiment (Table 1), suggests that most of the P was consumed by precipitation as vivianite. As determined by Mössbauer spectroscopy (Fig. 8), the MR-1 bioreduced magnetite contained a higher proportion of vivianite (8.2%) than did the CN32 bioreduced sample (6.5%), a result that is consistent with the relative intensity of the peaks corresponding to vivianite in the X-ray diffractograms in Fig. 6a and b. However, these results are in contrast with the greater amount of HCl-extractable Fe(II) in the CN32-reduced treatment (22.3 mM) compared to the MR-1 reduced magnetite (15.8 mM). The reasons for this discrepancy are unclear.

4.3. Biomineralization sequence during magnetite reduction

Thermodynamic calculations conducted by Fredrickson et al. (1998) for HFO reduction by CN32 in the bicarbonate-buffered medium indicated that the magnetite stability field would be encountered before that of siderite. A small amount of magnetite in the bicarbonate-buffered medium was indeed observed under TEM. However, the genetic relationship between magnetite and siderite, if it

existed, was not determined. In this study, biogenic magnetite from HFO reduction was used, and treated to remove unreduced HFO, as the starting material to maximize the probability of capturing the transformation dynamics. This study complements the work by Fredrickson et al. (1998) in that magnetite was biotically converted to siderite under similar experimental conditions. Furthermore, our microscopic evidence (i.e.,Figs. 3 and 4) definitively delineated that magnetite-to-siderite transition in bicarbonate buffer involved dissolution of magnetite and precipitation of siderite. The Mössbauer spectroscopy results also indicate that the biogenic vivianite resulted from the complete reduction of magnetite grains, a finding that is consistent with the dissolution–precipitation mechanism suggested by the TEM analyses of the biogenic magnetite (Fig. 3). A solid-state conversion would result in a different ρ and Mössbauer parameters. Although it has been suggested that magnetite reduction involves dissolution–precipitation (Kostka and Nealson, 1995), no direct evidence has been presented. This dissolution–precipitation mechanism is also consistent with crystallographic constraint. That is, structures of magnetite and siderite are so drastically different that it is not possible for the solid state conversion from one phase to the other.

The dissolution–precipitation mechanism has important implications for bacterial accessibility to structural Fe(III) in crystalline phases. Bacteria may have more ready access to structural Fe(III) in poorly crystalline oxides, where structural defects may be abundant. The presence of humic acid, or its analog AQDS, apparently can relieve the requirement for the direct contact between cell and oxide, and promote the Fe(III) reduction (Zachara et al., 1998; Fredrickson et al., 1998). Dissolution of magnetite and liberation of Fe(III), possibly as an amorphous Fe(III) oxide precipitate, may be involved in the magnetite reduction process, but additional work is required to establish whether an Fe(III) dissolution mechanism is operative.

Combining the current results with previous research (Fredrickson et al., 1998), the biomineralization sequence in the bicarbonate-buffered medium appears to be as follows: HFO → magnetite → siderite (or vivianite in the presence of P). In this study, we have provided direct evidence for biotransformation of magnetite to siderite and/or vivianite. Magnetite reduction has been shown to be pH sensitive. At low pH (5–6.5), magnetite reduction is thermodynamically favored (Kostka and Nealson, 1995). While the thermodynamics is less favorable at pH > 6.5, the overall free energy change is strongly influenced by the presence of Fe(II) complexing ligands such as bicarbonate and phosphate and by the precipitation of ferrous containing mineral phases (Fredrickson et al., 1998) that were not considered in the thermodynamic analysis.

As shown in this study, bacterial reduction of magnetite is dependent upon many factors including medium composition and organism type. It is possible that there are significant differences among the abilities of metal-reducing bacteria for reducing crystalline Fe oxides such as magnetite but a systematic analysis of these variations, to our knowledge, has not been done. The combination of pH, organism differences, and the thermochemical effects of secondary reactions may account for some of previous reports regarding the inability of some metal reducing bacteria to reduce magnetite (Lovley and Phillips, 1986; Lovley et al., 1993a,b; Roden and Lovley, 1993).

4.4. Implication for biogeochemical transformations

Magnetite is a major mineralogic component of banded iron formations (Walker, 1984), and ubiquitous in recent freshwater (Hilton et al., 1986; Maher and Taylor, 1988; Thouveny et al., 1994) and marine environments (Karlin and Levi, 1983; Kirschvink and Chang, 1984; Karlin et al., 1987; Shau et al., 1993). Microbial magnetite dissolution could have a significant impact on sediment and groundwater geochemistry, and rock magnetic properties. We have demonstrated that microbial reduction of magnetite is strongly influenced by pH, Eh, local microenvironment (aqueous solution composition) and strain of bacterium.

The ability of bacteria to utilize crystalline magnetite has far-reaching implications for microbial processes in sediments, especially in the subsurface where Fe(III) associated with Fe oxides may represent the largest mass of electron acceptor. Although the rates of in situ iron-reducing activity are not easily determined, laboratory-based evidence indicates that it is feasible in deep subsurface environ-

ments where both organic C and magnetite may be present. Magnetite dissolution and siderite formation is also of environmental importance. Metal oxides have been proposed as a means for disposal of radionuclide waste because these oxides have a high affinity for radionuclides. Dissolution of Fe oxides by bacteria would mobilize these constituents and release them to aquifer systems (Francis and Dodge, 1990). Alternatively, crystallization of siderite may incorporate some inorganic contaminants, such as Co(II) and Ni(II), into its structure, thus resulting in immobilization.

5. Conclusion

Biogenic and synthetic magnetite were reduced by *S. putrefaciens*. The extent of reduction and the nature of mineral products formed strongly depended on pH and aqueous phase composition. The extent of biogenic magnetite reduction in the bicarbonate-buffered medium was greater than that in the PIPES-buffered medium, probably via continuous removal of bioproduced Fe(II) by formation of siderite and vivianite. The biomineralization process in the presence of bicarbonate could be summarized as follows: HFO → magnetite → siderite (vivianite). Transformation from magnetite to siderite was accomplished through dissolution of magnetite and precipitation of siderite. Strain CN32 reduced more synthetic magnetite than biogenic magnetite, likely due to the difference in the reduction medium but also to the higher Fe(III) content of the synthetic magnetite. The extent of magnetite reduction was also impacted by growth conditions of the inoculum and strain type. Aerobically cultured cells reduced more magnetite than did anaerobically cultured cells although the reason for this is unknown. Under the same conditions, CN32 cells reduced more magnetite than MR-1. Vivianite formed in those media containing P. Bacteria were observed to become enshrouded in magnetite with time, possibly due to accumulation in a microbially produced exopolymer. The role of the polymer in attachment, reduction, and as a possible sink for Fe(II) is unknown but warrants further investigation.

Acknowledgements

The research was supported by the Department of Energy's (DOE) Office of Basic Energy Sciences, Geosciences Research Program under the management by Dr. Nick Woodward. We thank J.G. Goodhouse at the Department of Molecular Biology of the Princeton University for his technical assistance. Pacific Northwest National Laboratory is operated for the DOE by Battelle Memorial Institute under Contract DE-AC06-76RLO 1830. We thank Dr. David Boone of the Portland State University for providing *S. putrefaciens* CN32 to us from the Subsurface Microbial Culture Collection and Dr. Yuri Gorby for helpful discussions. We are grateful to Duane Moser and Kenneth Nealson for providing *S. putrefaciens* (*oniediensis*) MR-1, and Jim Amonette for the synthetic magnetite. We also wish to thank Joel Kostka and one anonymous reviewer for their insightful comments.

References

Arnold, R.G., DeChristina, T.J., Hoffman, M.R., 1988. Reductive dissolution of Fe(III) oxides by *Pseudomonas sp.* 200. Biotechnol. Bioeng. 32, 1081–1096.

Baedecker, M.J., Cozzarelli, I.M., Evans, J.R., Hearn, P.P., 1992. Authigenic mineral formation in aquifers rich in organic material. In: Kharaka, Y.K., Maest, A.S. (Eds.), Water–Rock Interaction. Proceedings of the 7th International Symposium on Water–Rock Interaction, Balkema, Rotterdam. pp. 257–261.

Bancroft, G.M., 1973. Mössbauer Spectroscopy: An Introduction for Inorganic Chemists and Geochemists. McGraw-Hill, London.

Cairns-Smith, A.G., Hall, A.J., Russell, M.J., 1992. Mineral theories of the origin of life and an iron sulfide example. Orig. Life Evol. Biosphere 22, 161–180.

de Durve, C., 1995. Vital Dust: Life as a Cosmic Imperative. Basic Books, New York, 362 pp.

Emerson, S., 1976. Early diagenesis in anaerobic lake sediments: chemical equilibria in interstitial waters. Geochim. Cosmochim. Acta 40, 925–934.

Emerson, S., Widmer, G., 1978. Early diagenesis in anaerobic lake sediments: II. Thermodynamic and kinetic factors controlling the formation of iron phosphate. Geochim. Cosmochim. Acta 42, 1307–1316.

Ferris, F.G., 1989. Metallic ion interactions with the outer membrane of Gram-negative bacteria. In: Beveridge, T.J., Doyle, R.J. (Eds.), Metal Ions and Bacteria. Wiley, New York, pp. 295–323.

Francis, A.J., Dodge, C.J., 1990. Anaerobic microbial remobilization of toxic metals co-precipitated with iron oxide. Environ. Sci. Technol. 24, 373–378.

Fredrickson, J.K., Zachara, J.M., Kennedy, D.W., Dong, H., Onstott, T.C., Hinman, N.W., Li, S., 1998. Biogenic iron mineralization accompanying the dissimilatory reduction of hydrous ferric oxide by a groundwater bacterium. Geochim. Cosmochim. Acta 62, 3239–3257.

Geesey, G.G., Jang, L., 1989. Interactions between metal ions and capsular polymers. In: Beveridge, T.J., Doyle, R.J. (Eds.), Metal Ions and Bacteria. Wiley, New York, pp. 325–357.

Gold, T., 1992. The deep, hot biosphere. Proc. Natl. Acad. Sci. U. S. A. 89, 6045–6049.

Granthan, M.C., Dove, P.M., DiChristina, T.J., 1997. Microbially catalyzed dissolution of iron and aluminum oxyhydroxide mineral surface coatings. Geochim. Cosmochim. Acta 61, 4467–4477.

Greenwood, N.N., Gibb, T.C., 1971. Mössbauer Spectroscopy. Chapman & Hall, London, Chapters 6 and 10.

Hilton, J., Lishman, J.P., Chapman, J.S., 1986. Magnetic and chemical characterization of a diagenetic magnetic mineral formed in the sediments of productive lakes. Chem. Geol. 56, 325–333.

Karlin, R., Levi, S., 1983. Diagenesis of magnetic minerals in recent haemipelagic sediments. Nature 303, 327–330.

Karlin, R., Lyle, M., Heath, G.R., 1987. Authigenic magnetite formation in suboxic marine sediments. Nature 326, 490–493.

Kazumi, J., Haggblom, M.M., Young, L.Y., 1995. Degradation of monochlorinated and nonchlorinated aromatic compounds under iron-reducing conditions. Appl. Environ. Microbiol. 61, 4069–4073.

Kirschvink, J.L., Chang, S.R., 1984. Ultra-fine grained magnetite in deep-sea sediments: possible bacterial magnetofossils. Geology 12, 559–562.

Kostka, J.E., Nealson, K.H., 1995. Dissolution and reduction of magnetite by bacteria. Environ. Sci. Technol. 29, 2535–2540.

Little, B., Wagner, P., Ray, R., Hart, K., Lavoie, D., Nealson, K., Aguilar, C., 1997. The role of biomineralization in microbiologically influenced corrosion. Biodegradation 9, 1–10.

Lovley, D.R., Phillips, E.J.P., 1986. Availability of ferric iron for microbial reduction in bottom sediments of the freshwater tidal Potomac River. Appl. Environ. Microbiol. 52, 751–757.

Lovley, D.R., Phillips, E.J.P., 1987. Rapid assay for microbially reducible ferric iron in aquatic sediments. Appl. Environ. Microbiol. 53, 1536–1540.

Lovley, D.R., Phillips, E.J.P., 1988. Novel mode of microbial energy metabolism: organic carbon oxidation coupled to dissimilatory reduction of iron or manganese. Appl. Environ. Microbiol. 54, 1472–1480.

Lovley, D.R., Baedecker, M.J., Lonergan, D.J., Cozzarelli, I.M., Phillips, E.J.P., Siegel, D.I., 1989. Oxidation of aromatic contaminants coupled to microbial iron reduction. Nature 339, 298–301.

Lovley, D.R., Lonergan, D.J., 1990. Anaerobic oxidation of toluene, phenol, and ρ-cresol by the dissimatory iron-reducing organism, GS-15. Appl. Environ. Microbiol. 56, 1858–1864.

Lovley, D.R., 1991. Magnetite formation during microbial dissimilatory iron reduction. In: Frankel, R.B., Blakemore, R.P. (Eds.), Iron Biominerals. Plenum, New York, pp. 151–166.

Lovley, D.R., Giovannoni, S.J., White, D.C., Champine, J.E., Phillips, E.J.P., Gorby, Y.A., Goodwin, S., 1993a. *Geobacter metallireducens* gen. nov., a microorganism capable of coupling the complete oxidation of organic compounds to the reduction of iron and other metals. Arch. Microbiol. 159, 336–344.

Lovley, D.R., Roden, E.R., Phillips, E.J.P., Woodward, J.C., 1993b. Enzymatic iron and uranium reduction by sulfate-reducing bacteria. Mar. Geol. 113, 41–53.

Lovley, D.R., 1995. Bioremediation of organic and metal contaminants with dissimilatory metal reduction. J. Ind. Microbiol. 14, 85–93.

Lovley, D.R., Coates, J.D., Blunt-Harris, E.L., Phillips, E.J.P., Woodward, J.C., 1996. Humic substances as electron acceptors for microbial respiration. Nature 382, 445–448.

Lovley, D.R., Fraga, J.L., Blunt-Harris, E.L., Hayes, L.A., Phillips, E.J.P., Coates, J.D., 1998. Humic substances as a mediator for microbially catalyzed metal reduction. Acta Hydrochim. Hydrobiol. 26, 152–157.

Maher, B.A., Taylor, R.M., 1988. Formation of ultra-fine-grained magnetite in soils. Nature 336, 368–370.

McKay, D.S., Gibson, E.K., Thomas-Keprta, K.L., Vali, H., Romanek, C.S., Clement, S.J., Chillier, X.D.F., Maechling, C.R., Zare, R.N., 1996. Search for past life on Mars: possible relic biogenic activity in Martian meteorite ALH84001. Science 273, 924–930.

Mortimer, R.J.G., Coleman, M.L., Rae, J.E., 1997. Effect of bacteria on the elemental composition of early diagenetic siderite: implication for paleoenvironmental interpretations. Sedimentology 44, 759–765.

Nealson, K.H., Saffarini, D., 1994. Iron and manganese in anaerobic respiration: environmental significance, physiology, and regulation. Annu. Rev. Microbiol. 48, 311–343.

Nealson, K.H., Little, B., 1997. Breathing manganese and iron: solid-state respiration. Adv. Appl. Microbiol. 45, 213–239.

Olsen, S.R., Sommers, L.E., 1982. Phosphorous. Methods of Soil Analysis: Part 2. Chemical and Microbiological Properties. In: Page, A.L., Miller, R.H., Keeney, D.R. (Eds.), American Society for Agronomypp. 403–430.

Obuekwe, C.O., Westlake, D.W.S., Cook, F.D., Costerton, J.W., 1981. Surface changes in mild steel coupons from the action of corrosion-causing bacteria. Appl. Environ. Microbiol. 41, 766–774.

Pye, K., Dickson, J.A.D., Schiavon, N., Coleman, M.L., Cox, M., 1990. Formation of siderite-Mg–calcite-iron sulphide concretions in intertidal marsh and sandflat sediments, north Norfolk, England. Sedimentology 37, 325–343.

Rancourt, D.G., Ping, J.Y., 1991. Voigt-based methods for arbitrary shape static hyperfine parameter distributions in Mössbauer spectroscopy. Nucl. Instrum. Methods Phys. Res., Sect. B 58, 85–87.

Roden, E.E., Lovley, D.R., 1993. Dissimilatory Fe(III) reduction by the marine microorganism *Desulfuromonas acetoxidans*. Appl. Environ. Microbiol. 59, 734–742.

Roden, E.E., Zachara, J.M., 1996. Microbial reduction of crys-

talline Fe(III) oxides: influence of oxide surface area and potential for cell growth. Environ. Sci. Technol. 30, 1618–1628.

Shau, Y., Peacor, D.R., Essene, E.J., 1993. Formation of magnetite single-domain magnetite in ocean ridge basalts with implications for sea floor magnetism. Science 261, 343–345.

Sparks, N.H.C., Mann, S., Bazylinski, D.A., Lovley, D.R., Jannasch, H.W., Frankel, R.B., 1990. Structure and morphology of magnetite anaerobically produced by a marine magnetotactic bacterium and a dissimilatory iron-reducing bacterium. Earth Planet. Sci. Lett. 98, 14–22.

Schwertmann, U., Cornell, R.M., 1991. Iron Oxides in the Laboratory. VCH, New York, 137 pp.

Thouveny, N., de Beaulieu, J.L., Bonifay, E., Creer, K.M., Guiot, J., Icole, M., Johnson, S., Jouzel, J., Reille, M., Williams, T., Williamson, D., 1994. Climate variations in Europe over the past 140 kyr deduced from rock magnetism. Nature 371, 503.

Urrutia, M.M., Roden, E.E., Fredrickson, J.K., Zachara, J.M., 1998. Microbial and surface chemistry controls on reduction of synthetic Fe(III) oxide minerals by the dissimilatory iron-reducing bacterium *Shewanella alga*. Geomicrobiol. J. 15, 269–291.

Vandenberghe, R.E., Hus, J.J., Grave, E.De., 1998. Evidence from Mössbauer spectroscopy of neo-formation of magnetite/maghemite in soils of loess/palesol sequences in China. Hyperfine Interact. 117, 359–369.

Vargas, M., Kashefi, K., Blunt-Harris, E.L., Lovley, D.R., 1998. Microbiological evidence for Fe(III) reduction on early Earth. Nature 395, 65–67.

Walker, J.C.G., 1984. Suboxic diagenesis in banded iron formations. Nature 309, 340–342.

Walker, J.C.G., 1987. Was the Archaean biosphere upside down? Nature 329, 710–712.

Zachara, J.M., Fredrickson, J.K., Fredrickson, L., Fredrickson, S.-W., Kennedy, D.W., Smith, S.C., Gassman, P.L., 1998. Bacterial reduction of crystalline Fe^{3+} oxides in single phase suspensions and subsurface materials. Am. Mineral. 83, 1426–1443.